

RECENT QCD RESULTS FROM CDF

STEFANO LAMI*

The Rockefeller University, 1230 York Avenue, New York, NY 10021, USA
E-mail: lami@fnal.gov

The measurement of the inclusive jet cross-section at $\sqrt{s}=1960$ GeV is compared to NLO QCD predictions and to Run 1 data. Results on single diffractive di-jet production are also presented as an example of the CDF forward physics program.

1. Introduction

The CDF experiment is currently accumulating large samples of data during Run 2 at the Tevatron, and with high statistics it will be able to extract the fundamental parameter of QCD, α_s , and the parton distribution functions (PDFs), from several different processes. This short contribution focuses on recent results on the inclusive jet cross-section, an important measurement in which to look for new physics beyond the Standard Model, and on single diffractive di-jet production as an example of the extensive forward physics program in Run 2.

2. Inclusive Jet Production

The measurement of the inclusive jet cross-section at the Tevatron probes a distance scale of $\sim 10^{-19}$ m, the smallest distance currently probed in experimental particle physics. There was great interest in Run 1 when initial inclusive jet cross-section measurements showed an excess at high jet transverse energy E_T over NLO theoretical predictions using the available PDFs, since a deviation at high E_T could indicate the presence of new physics processes or quark compositeness¹. A global PDF analysis by the CTEQ group demonstrated that such an excess can be explained in terms of a larger than expected gluon distribution at high x^2 . Recent PDFs, like CTEQ6, extracted from a larger data sample that includes CDF and DØ Run 1 measurements, have an increased high- x gluon contribution, but

*On behalf of the CDF Collaboration.

still with a big uncertainty which we hope will be reduced by Run 2 jet measurements.

The data set used in this analysis corresponds to an integrated luminosity of 177 pb^{-1} collected in 2002-03. This first Run 2 measurement, at a center of mass energy of 1.96 TeV, extends the Run 1 kinematic range of the jet transverse energy E_T by about 150 GeV (see Fig. 1). Reconstruction

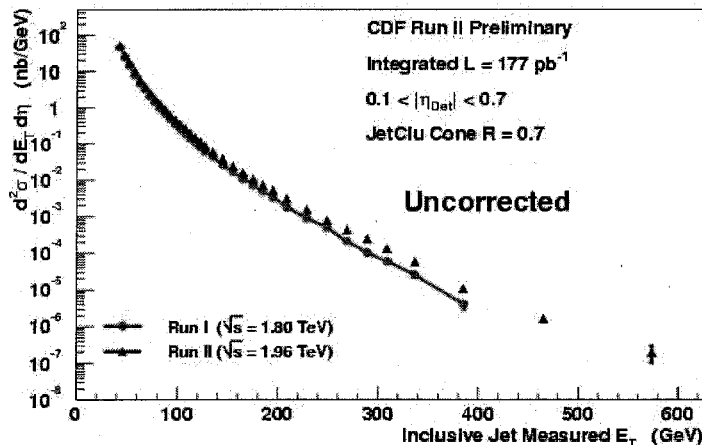


Figure 1. Run 2 raw data compared to Run 1 raw data.

of jets is limited to the central calorimeter for the time being, using a cone algorithm with radius $R = (\Delta\phi^2 + \Delta\eta^2)^{1/2}$. The underlying event energy from the fragmentation of spectator partons is subtracted. Jet energies are not corrected for parton energy lost outside the cone, as this effect is supposed to be modeled by NLO QCD calculations.

The jet E_T spectrum has to be corrected for detector and smearing effects caused by finite E_T resolution with an ‘unsmearing procedure’ before comparing it to NLO QCD predictions. To evaluate the jet energy response, one needs to know the calorimeter response to single particles, and the momentum spectrum of particles in a jet (fragmentation function). The former was measured from test-beam data and isolated tracks in minimum bias events; the latter was measured using the CDF central tracker.

Systematic uncertainties arise from our understanding of the calorimeter response to jets, plus jet fragmentation functions and jet energy resolution. Other uncertainties are related to underlying event subtraction and normalization. All these uncertainties are functions of jet E_T but independent of each other. The combined systematic uncertainty varies from 30% at 40 GeV to 50% at 550 GeV (see Fig. 2).

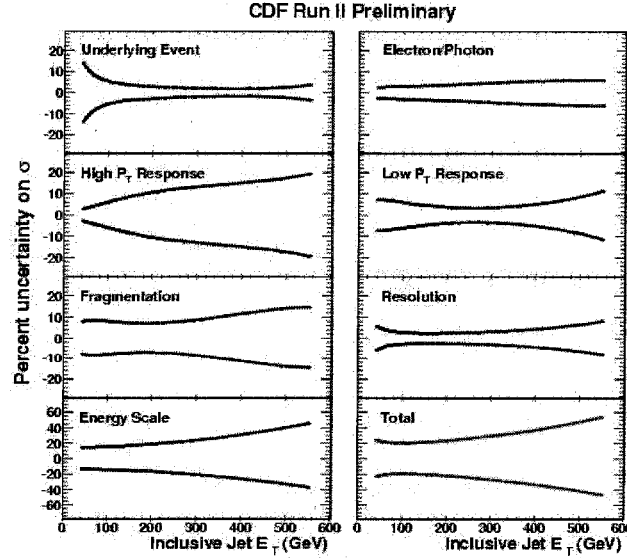


Figure 2. Percentage error on the corrected cross-section resulting from the individual contributions to the systematic error.

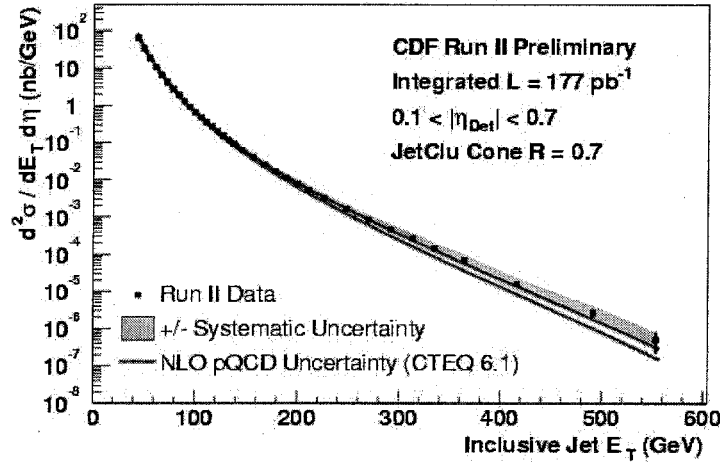


Figure 3. Run 2 data compared to NLO QCD prediction. The error band shows the change in the cross-section due to the 3% energy scale shift.

The unsmearred data are compared with NLO QCD prediction in Fig. 3. The theoretical uncertainty due to PDFs is indicated by the area within the two solid lines, while the shaded band represents the total experimental systematic error, dominated by the energy scale uncertainty. In Fig. 4 data are divided by theory on a linear scale. There is some indication of the data

being below the theory at low E_T and somewhat above at higher E_T , but overall the agreement is good. Work is in progress to reduce the current

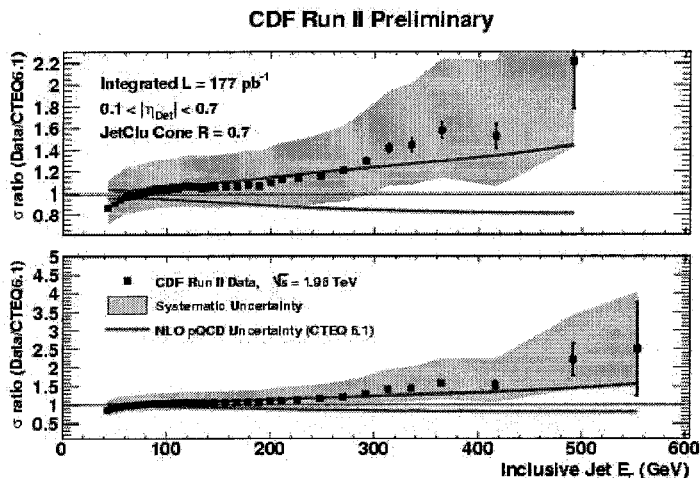


Figure 4. Data divided by the theoretical prediction (upper plot is a zoom excluding the last bin of lower plot).

energy scale uncertainty, to extend the analysis to forward jets using the new Plug calorimeter, and to use additional jet algorithms like MidPoint, an improved version of Run 1 cone algorithm designed to satisfy theoretical issues, and the K_T algorithm, widely used at LEP.

3. Single Diffractive Di-Jet Production

Building bridges between QCD and Regge theory has become a hot topic in recent years thanks to hard diffraction processes, which merge a high transverse momentum parton scattering with diffractive event features. Figure 5 shows a single diffractive di-jet production diagram. The signature is a

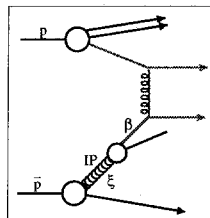


Figure 5. Single diffractive di-jet production.

leading antiproton, which escapes the collision intact, losing only a small momentum fraction ξ to the Pomeron; a parton from the Pomeron scatters with a parton from the proton resulting in two high E_T jets. The leading antiproton is detected by a Roman Pot Spectrometer, and the associated forward rapidity gap may be tagged by Beam Shower counters installed around the beam-pipe; the two jets are reconstructed by the central calorimetry. The addition of two Mini-Plug calorimeters extends the calorimetry coverage into the forward direc-

tion and helps providing a clean separation between diffractive and non-diffractive events.

The diffractive structure function can be investigated by comparing single diffractive and non-diffractive di-jet production, as the ratio of their rates is proportional to the ratio of the corresponding structure functions and can be studied as a function of the Bjorken variable $x = \beta\xi$ of the struck parton in the antiproton, where β is the Pomeron momentum fraction carried by its struck parton. The antiproton momentum loss fraction ξ is measured using all calorimeter towers including MiniPlugs, and is plotted in Fig. 6. Single diffraction and background regions are selected according to the measured ξ values. Large ξ values - around $\xi=1$ - correspond to non-diffractive events where the antiproton breaks up and loses completely its initial momentum. The plateau at low ξ values comes from the diffractive events where very little energy is measured in the antiproton forward region, and the declining at very small ξ values occurs in the region where the Roman Pot acceptance decreases. The ratio of diffractive to non-diffractive

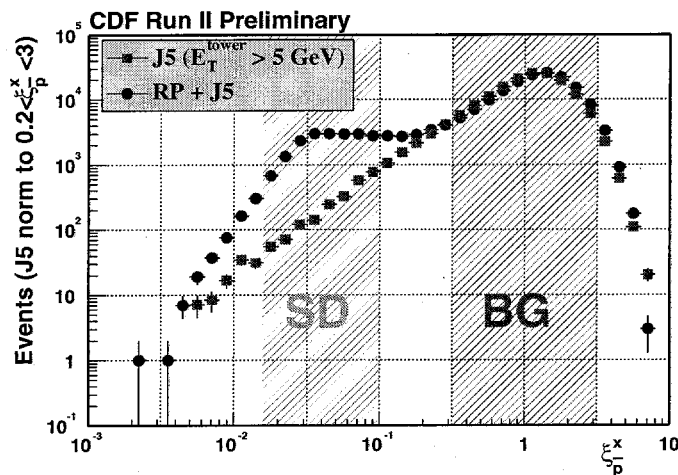


Figure 6. Momentum loss of the antiproton ξ distribution for the diffractive (circles) and the non-diffractive (squares) trigger samples.

di-jet production rates is plotted in Fig. 7 as a function of the Bjorken scaling variable x of the struck parton in the antiproton. For each event, x is evaluated from the E_T and pseudorapidity η of the jets within $|\eta| < 2.5$. In LO QCD this ratio is the ratio of the diffractive to non-diffractive parton densities of the antiproton in di-jet production. Results from Run 2 (circles) are in good agreement with Run 1 measurements (squares)³. Run 2 results are also shown for two separate ξ bins, multiplied and divided by

a factor 10, respectively. Another preliminary result, presented in Fig. 8,

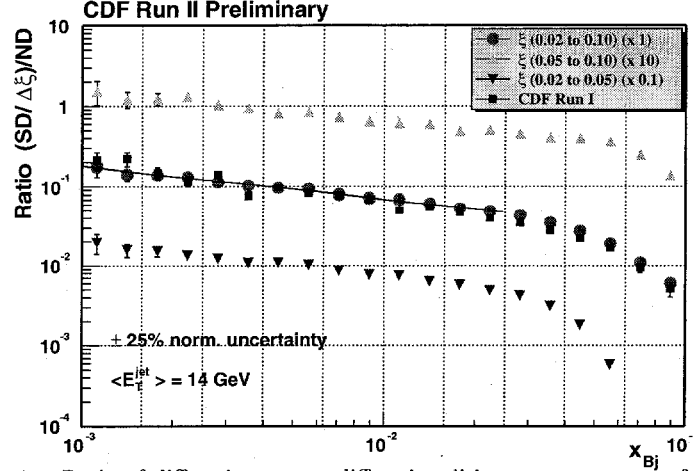


Figure 7. Ratio of diffractive to non-diffractive di-jet event rates as a function of x . Run 2 data (circles) are compared to Run 1 data (squares).

shows that the ratio does not depend strongly on $E_T^2 = Q^2$ in the range from $Q^2 = 100$ up to $Q^2 = 1600$ GeV^2 . This result indicates that the Q^2 evolution of the Pomeron is similar to that of the proton.

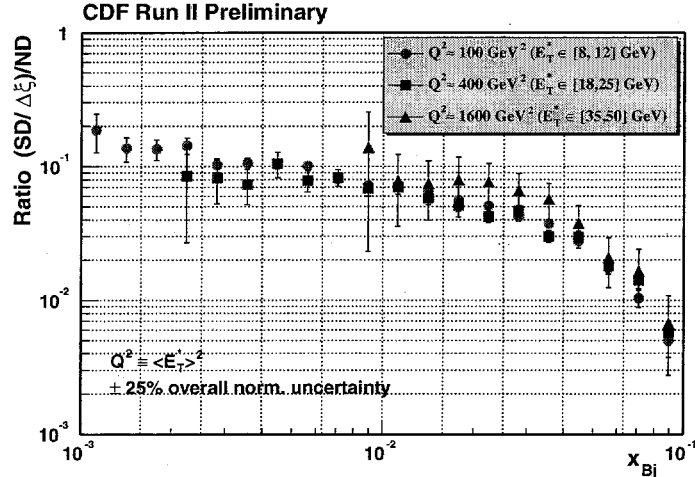


Figure 8. Ratio of diffractive to non-diffractive di-jet event rates as a function of x , plotted for different Q^2 regions.

References

1. T. Affolder *et al.*, *Phys. Rev.* **D64**, 032001 (2001).
2. H.L. Lai *et al.*, *Phys. Rev.* **D55**, 1280 (1997); *Eur. Phys. J.* **C12**, 375 (2000).
3. T. Affolder *et al.*, *Phys. Rev. Lett.* **84**, 5043 (2000).